The proapoptotic and antimitogenic protein p66SHC acts as a negative regulator of lymphocyte activation and autoimmunity

Francesca Finetti,[1] Michela Pellegrini,[1] Cristina Ulivieri,[1] Maria Teresa Savino,[1] Eugenio Paccagnini,[1] Chiara Ginanneschi,[2] Luisa Lanfrancone,[3] Pier Giuseppe Pelicci,[3] and Cosima T. Baldari[1]

[1]Department of Evolutionary Biology, University of Siena, Siena; [2]Department of Human Pathology and Oncology, Policlinico Le Scotte, University of Siena, Siena; and [3]Department of Molecular Oncology, European Institute of Oncology, Milan, Italy

The *ShcA* locus encodes 3 protein isoforms that differ in tissue specificity, subcellular localization, and function. Among these, p66Shc inhibits TCR coupling to the Ras/MAPK pathway and primes T cells to undergo apoptotic death. We have investigated the outcome of p66Shc deficiency on lymphocyte development and homeostasis. We show that p66Shc$^{-/-}$ mice develop an age-related lupus-like autoimmune disease characterized by spontaneous peripheral T- and B-cell activation and proliferation, autoantibody production, and immune complex deposition in kidney and skin, resulting in autoimmune glomerulonephritis and alopecia. p66Shc$^{-/-}$ lymphocytes display enhanced proliferation in response to antigen receptor engagement in vitro and more robust immune responses both to vaccination and to allergen sensitization in vivo. The data identify p66Shc as a negative regulator of lymphocyte activation and show that loss of this protein results in breaking of immunologic tolerance and development of systemic autoimmunity. (Blood. 2008;111:5017-5027)

Introduction

The Shc protein family includes 4 members, ShcA, ShcB, ShcC, and RaLP.[1,2] ShcA is expressed as 3 isoforms of 52, 46, and 66 kDa, which display the PTB-CH1-SH2 Shc family signature, preceded in p66Shc by a CH2 domain containing a phosphorylatable serine (Ser36)[3] and a cytochrome *c*–binding region within the CH2-PTB domains.[4] In addition to structural differences, p52Shc/p46Shc differ from p66Shc in expression and function. The shorter isoforms are constitutively and ubiquitously expressed, whereas p66Shc expression is regulated by an alternative promoter[5] and is tissue restricted.[6] ShcA isoforms differ also in their subcellular localization and function. p52Shc is a cytosolic protein acting as adaptor in pathways triggered by surface receptors controlling proliferation, chemotaxis, and survival.[7,8] p46Shc localizes to mitochondria, where it subserves an unknown function.[9] On the other hand, p66Shc is expressed as 2 pools, one cytosolic and the other mitochondrial, and is endowed with antimitogenic and proapoptotic activities. Indeed, p66Shc inhibits activation of the Ras/MAPK pathway by tyrosine kinase receptors and the T-cell antigen receptor (TCR) by competing with p52Shc. Furthermore, in fibroblasts, p66Shc participates in oxidative stress–induced apoptosis by triggering the mitochondrial pathway as a p53 target.[10]

p66Shc-mediated apoptosis is dependent on Ser36 phosphorylation, which is mediated by PKCβ and required for p66Shc translocation from the cytosol to mitochondria by the prolyl-isomerase Pin1.[11] In mitochondria, p66Shc is maintained in an inactive state within a high-molecular-mass complex, which includes the TIM-TOM import complex and Hsp70. Following proapoptotic stimulation, p66Shc is released and acquires the capacity to oxidize cytochrome *c* and catalyze H_2O_2 production, leading to mitochondrial dysfunction, opening of the permeability transition pore (PTP), and apoptosis.[4,12] Moreover, p66Shc modulates the levels of reactive oxygen species (ROSs) by suppressing activation of FKHRL1, a forkhead transcription factor that controls catalase expression and is implicated as such in H_2O_2 scavenging.[13] Alterations in oxidative metabolism in p66Shc$^{-/-}$ fibroblasts, characterized by decreased mitochondria-dependent energy generation and increased aerobic glycolysis,[14] also contribute to the reduction in ROS levels observed in these cells. In agreement with the capacity of p66Shc to increase intracellular ROSs, *p66Shc* ablation in the mouse results in life-span extension and resistance to oxidants,[15] as well in protection from oxidant-related diseases, such as high-fat diet–induced atherogenesis[16] and oxidant-induced diabetic glomerulopathy.[17]

T cells express low p66Shc levels due to partial methylation of a CpG island within the gene promoter.[5] T-cell treatment with proapoptotic stimuli results in enhanced p66Shc expression, which correlates with promoter demethylation.[18] Similarly to fibroblasts, p66Shc expression in T cells antagonizes activation of the Ras/MAPK pathway, at least in part by competitive inhibition of p52Shc, and attenuates proliferative responses to TCR agonists. Furthermore, p66Shc enhances T-cell susceptibility to apoptosis through 2 independent mechanisms.[19] Of these, the first involves dissipation of mitochondrial transmembrane potential and cytochrome *c* release due to an imbalance in the expression levels of proapoptotic/antiapoptotic Bcl-2 family members,[19] while the second involves Ca^{2+} deregulation due to decreased expression and activity of plasma membrane Ca^{2+} ATPases through the ROS-elevating activity of p66Shc.[20]

Submitted December 22, 2007; accepted March 7, 2008. Prepublished online as *Blood* First Edition paper, March 11, 2008; DOI 10.1182/blood-2007-12-130856.

The online version of this article contains a data supplement.

The publication costs of this article were defrayed in part by page charge payment. Therefore, and solely to indicate this fact, this article is hereby marked "advertisement" in accordance with 18 USC section 1734.

The defects found in p66Shc$^{-/-}$ T cells, as well as their enhanced proliferative responses to TCR agonists, suggest a potential impact of p66Shc deficiency in immune repertoire selection and lymphocyte homeostasis. Here we show that p66Shc$^{-/-}$ mice harbor spontaneous lymphocyte activation and develop a lupus-like autoimmune disease. These pathological features correlate with a hyperreactivity of p66Shc$^{-/-}$ lymphocytes to antigen receptor (AgR) triggering, both in vitro and in vivo. The data identify p66Shc as a novel key negative regulator of TCR and BCR signaling.

Methods

Mice

p66Shc$^{-/-}$ mice[15] and control age-matched 129sv mice (Charles River Italia, Calco, Italy) were used. Age groups were either 6 weeks (young mice) or 6 to 12 months (aged mice). Mice were maintained in the animal facilities at the University of Siena (Siena, Italy) and the European Institute of Oncology–Italian Foundation for Cancer Research (FIRC) Institute of Molecular Oncology (IEO-IFOM, Milan, Italy), housed in a light (07:00–19:00)– and temperature (18°C-22°C)–controlled environment, and food (Global diet 2018; Mucedola, Settimo Milanese, Italy) and water were provided ad libitum. Animal experiments were done in agreement with the Guiding Principles for Research Involving Animals and Human Beings and approved by the local ethics committees.

Splenic cell purification and immunoblotting

Splenic cells were purified by immunomagnetic sorting using anti-panB and anti-panT antibody-conjugated beads (Dynal Biotech, Oslo, Norway) and checked for purity (consistently $> 90\%$) by flow cytometry with fluorochrome-conjugated anti-CD3/anti-CD22 mAbs. Monocytes were purified by adherence from single-cell suspensions from spleen. In some experiments, splenic B cells were activated using different concentrations of goat F(ab^1)$_2$ fragment to mouse IgM (Cappel; MP Biomedicals Europe, Brussels, Belgium) followed by incubation at 37°C for 5 minutes. Cells (5×10^6/sample) were lysed in 3% Triton X-100 in 20 mM Tris-HCl (pH 8), 150 mM NaCl (in the presence of a protease inhibitor cocktail). Shc expression was analyzed by immunoblot of postnuclear supernatants with polyclonal anti-SH2 antibodies (Upstate Biotechnology, Boston, MA) and secondary peroxidase-labeled antibodies (GE Healthcare, Little Chalfont, United Kingdom) using a chemiluminescence detection system (Pierce, Rockford, IL). Erk phosphorylation was detected using a phosphospecific antibody (Cell Signaling Technology, Beverly, MA). Control anti-Erk antibodies were purchased from Santa Cruz Biotechnology (Santa Cruz, CA). Immunoblots were quantified by laser densitometry (Kodak Digital Science Electrophoresis Documentation and Analysis System 120; Kodak, Rochester, NY).

Flow cytometry

Mice were killed by cervical dislocation. Single-cell suspensions were prepared from thymus, lymph nodes and spleen using cell strainer filters (BD Falcon; BD Biosciences Europe, Erembodegem, Belgium). Peripheral blood was obtained by tail bleeding using heparin as anticoagulant and subjected to flow cytometry after hypotonic lysis of erythrocytes. Bone marrow was obtained from femurs by flushing with RPMI, 7.5% FCS. Single-cell suspensions were prepared by gentle pipetting.

CD3, CD4, CD8, CD22, CD25, CD69, CD5, IgM, and IgD surface expression was analyzed by flow cytometry using FITC- or PE-conjugated antibodies (BD Biosciences Italia SpA, Milan, Italy; eBiosciences, San Diego, CA).

Mouse splenic B-cell proliferation was measured by flow cytometric analysis of carboxyfluorescein succinimidyl ester (CFSE)–labeled cells as described.[19] Cells were resuspended at 20×10^6/mL in PBS and stained with 10 μM CFSE (Molecular Probes Europe BV, Leiden, The Netherlands) for 8 minutes at room temperature. Cells were subsequently washed twice in RPMI, 7.5% FCS, resuspended at 5×10^6/mL, and activated with 30 μg/mL goat F(ab^1)$_2$ fragment to mouse IgM (Cappel). Cells were analyzed by flow cytometry 48, 72, and 96 hours after stimulation.

Flow cytometry was carried out using a FACScan flow cytometer (Becton Dickinson, San Jose, CA). Data were acquired using CellQuest and analyzed and plotted using Flowjo (TreeStar, Ashland, OR).

Tetanus toxoid immunization, serum processing, and ELISA

Six-month-old mice were intraperitoneally immunized 4 times with 2 μg TT in 100 μL PBS (kindly provided by F. Berti; Novartis Vaccines, Siena, Italy) at days 1, 21, 35, and 42. Seven days after the last immunization serum samples were collected and TT-specific antibody titers determined by enzyme-linked immunosorbent assay (ELISA). Specifically, flat-bottom 96-well ELISA plates (Greiner Bio-One, Frickenhausen, Germany) were coated with 0.3 μg/well TT and incubated at 4°C overnight. Plates were washed and incubated with blocking buffer (0.05% Tween 20, 0.02% NaN_3 in PBS) for 2 hours at 37°C, and 100 μL immune serum was applied as a 1:10 000 dilution in PT buffer (0.05% Tween 20 in PBS). After one wash, wells were coated with 100 μL anti–mouse IgG peroxidase-linked antibody (GE Healthcare) in PT buffer, and plates were incubated for 2 hours at 37°C. Color was developed with 100 μL/well stabilized tetramethilbenzidine (Biosource Europe SA, Nivelles, Belgium). The reaction was stopped by addition of 100 μL/well STOP solution (Biosource Europe SA). Absorbance was measured using a microplate reader (model 680; Bio-Rad, Hercules, CA) at 450 nm.

Serum antibodies specific for dsDNA were quantified by ELISA using a semiquantitative kit (Alpha-Diagnostic, San Antonio, TX).

Serum immunoglobulin levels were determined by ELISA using a clonotyping system-AP and a mouse immunoglobulin panel (Southern Biotechnology Associates, Birmingham, AL).

Delayed-type hypersensitivity reaction (DTH)

Mice were sensitized with a 3% 2,4,6-trinitrochlorobenzene (TNCB; Sigma Aldrich Italia, Milano, Italy) solution (4:1 acetone–olive oil) applied to the clipped abdomen. Six days later, mice were challenged by applying 10 μL 1% TNCB solution (9:1 acetone–olive oil) to both sides of one ear. Ear swelling was assessed 24 hours later using a micrometer (ALPA, Milano, Italy) and was expressed as thickness of challenged ear minus thickness of unchallenged ear plus or minus SD as described.[21]

Tissue processing and histology

For hematoxylin and eosin (H&E), Giemsa, or periodic acid-Schiff (PAS) staining, tissue fragments (spleen, kidney, or skin) were fixed in 10% formalin for 24 hours, embedded in paraffin, sectioned (5 μm), and stained using standard techniques. The tissues were visualized on a Zeiss microscope (Axiovert 200; Göttingen, Germany) equipped with a digital camera (InfinityX; Lumenera, Ottawa, ON).

For immunofluorescence, tissue fragments (kidney or skin) were embedded in Tissue-Tek OCT compound, flash-frozen in liquid nitrogen, and sectioned with a cryostat. Sections were stained with FITC-conjugated goat anti–mouse immunoglobulins (DAKO, Glostrup, Denmark) and visualized by fluorescence microscopy on a Leica DMRB microscope (Heidelberg, Germany) equipped with a standard camera (using Kodak T-MAX 400 film) or a digital camera (AxioCam MRc5; Zeiss). Images were processed using the digital imaging software AxioVision (Zeiss).

Kidney or skin tissue fragments were also prepared using standard procedures for conventional electron microscopy. Ultrathin sections (70 nm) were routinely stained with uranyl acetate and lead citrate and observed with a Philips CM10 transmission electron microscope (Andover, MA) with an electron accelerating voltage of 80 kV. Skin ultrathin sections were also

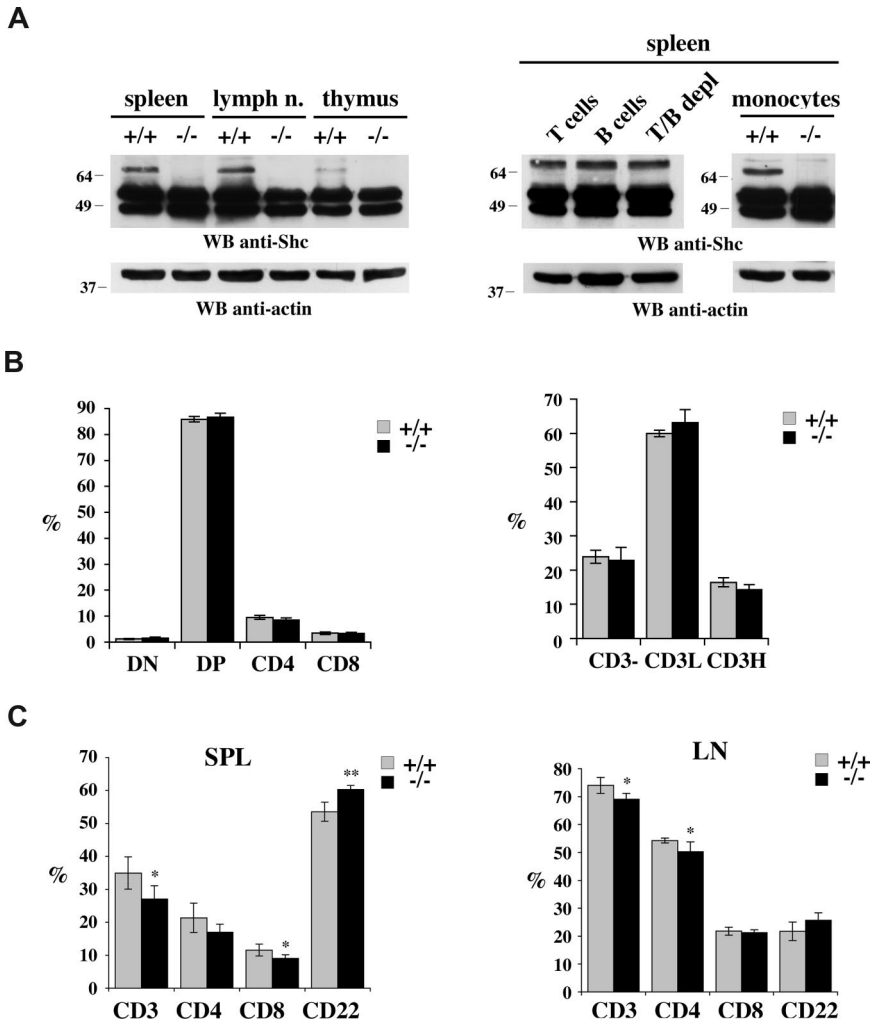

Figure 1. Normal lymphocyte development in 1-month-old p66Shc$^{-/-}$ mice. (A, left) Immunoblot analysis with anti-Shc antibodies of spleen, lymph nodes, and thymus postnuclear supernatants from untreated age-matched control (+/+) or p66Shc$^{-/-}$ (−/−) mice. (Right) Immunoblot with anti-Shc antibodies of postnuclear supernatants from splenocytes from wild-type mice purified by Immunomagnetic sorting with anti-panB, anti-panT or negatively sorted using anti-panB plus anti-panT antibody-conjugated magnetic beads, as well as from splenic monocytes purified by adherence. Control blots of the same filters with antiactin mAb are shown below. Representative experiments are shown (n ≥ 3). (B) Flow cytometric analysis of thymocytes from 6-week-old control (+/+) or p66Shc$^{-/-}$ (−/−) mice stained with anti-CD4/anti-CD8 and anti-CD3 fluorochrome-conjugated mAb. On the left, the histograms show the percentage (± SD) of double-negative (DN), double-positive (DP), or single-positive thymocytes for CD4 and CD8 expression. On the right the histogram shows the levels of CD3 expression: not expressed (CD3−) and with low (CD3L) or high (CD3H) expression. For each sample, fluorescence was analyzed on gated cells with forward and side light scatter properties of lymphocytes (n = 5). (C) Cells from spleen and lymph nodes of 6-week-old control (+/+) or p66Shc$^{-/-}$ (−/−) mice were stained with anti-CD3/anti-CD22 and anti-CD4/anti-CD8 fluorochrome-conjugated mAb and analyzed by flow cytometry. The histograms show the percentage (± SD) of single-positive cells in spleen (left) and lymph nodes (right) analyzed on gated lymphocyte populations (n = 5; *$P < .05$; **$P < .01$).

stained using standard techniques with toluidine blue and visualized on a Zeiss microscope (Axiovert 200).

Proteinuria analysis

Proteinuria was measured in a semiquantitative way using Combur 10 test (Roche Diagnostic, Milan, Italy). Mice were scored as positive for proteinuria when protein levels exceeded 100 mg/dL defined by the colorimetric test.

Statistical analyses

Mean values, standard deviation values, and Student *t* test (unpaired) were calculated using Microsoft Excel (Redmond, WA). A level of *P* less than .05 was considered statistically significant.

Results

Age-related alterations in lymphocyte populations in p66Shc$^{-/-}$ mice

We have previously reported that p66Shc is constitutively expressed, albeit at low levels compared with p52/p46Shc, in mouse thymocytes and splenic T cells.[19] The analysis was extended to lymph nodes, where p66Shc was also detected (Figure 1A left). Immunoblot analysis of immunomagnetically sorted splenocytes showed that p66Shc is expressed not only in T cells, but also in B cells (Figure 1A right). Furthermore, p66Shc was found in splenocytes depleted of both T and B cells, suggesting that p66Shc may be expressed both in the lymphoid and in the myeloid lineage. Expression of p66Shc in purified mouse splenic monocytes was indeed observed (Figure 1A right). No expression was detected in the bone marrow (data not shown).

The potential role of p66Shc in lymphocyte development was assessed by flow cytometric analysis of single-cell suspensions of thymus, spleen, and lymph nodes of both young (6-week old) and aged (12-month-old) p66Shc$^{-/-}$ mice. The CD4/CD8 surface profile showed that thymic development was unaffected by p66Shc deficiency (Figure 1B left; Figure S1A, available on the *Blood* website; see the Supplemental Materials link at the top of the online article). Analysis of CD3 (T-cell marker) and CD22 (B-cell marker) surface expression on single-cell suspensions from spleen and lymph nodes revealed a modest alteration in the proportions of T and B cells in young p66Shc$^{-/-}$ mice compared with controls (Figure 1C). The differences were more pronounced in the spleens of aged mice, where a decrease in the proportion of CD3$^+$ splenocytes, which affected both CD4$^+$ and CD8$^+$ cells, and an increase in the proportion of CD22$^+$ splenocytes were observed (Figure 2A left). Analysis of IgM/IgD surface expression of

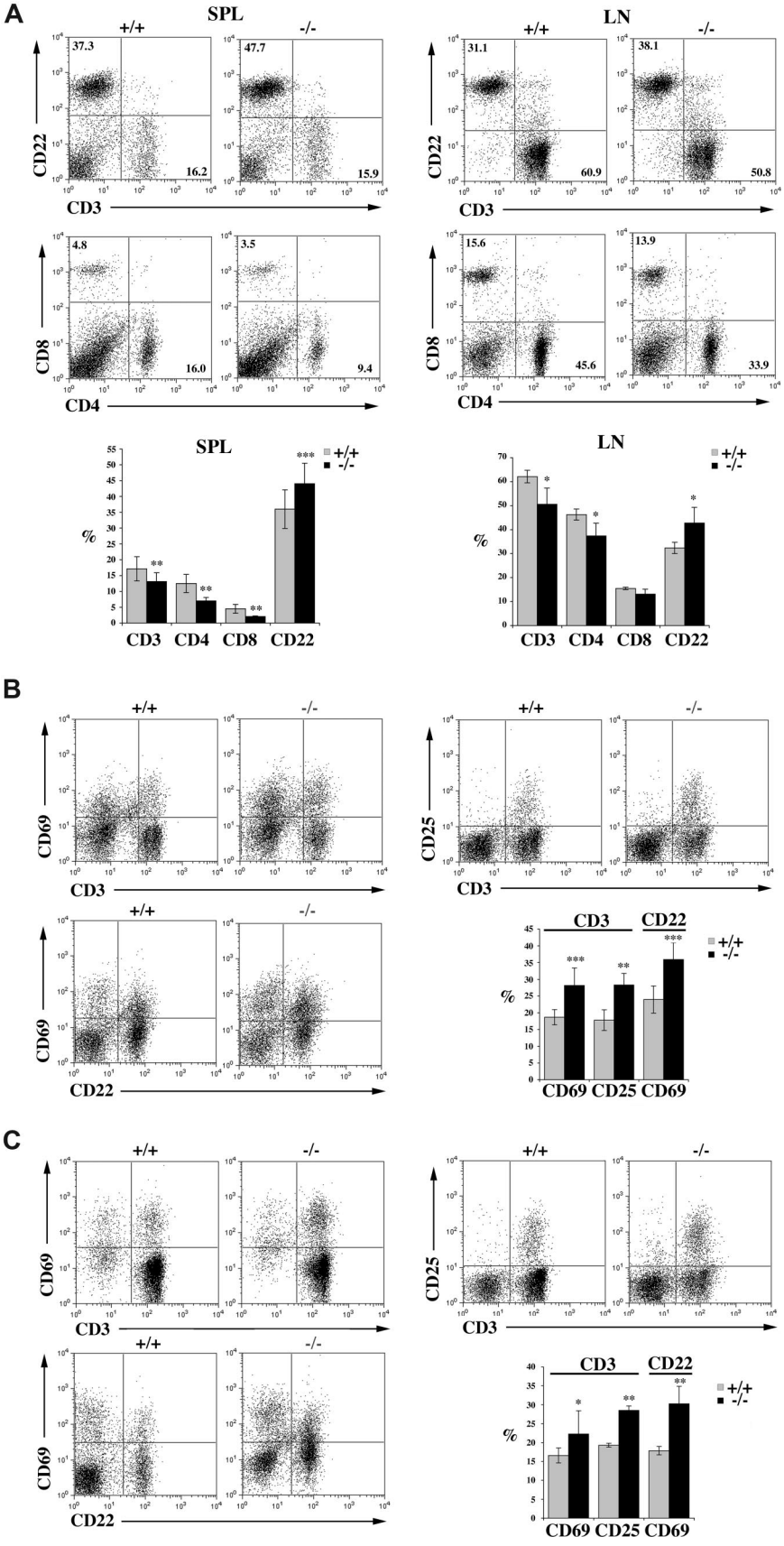

Figure 2. Spontaneous peripheral lymphocyte activation in p66Shc$^{-/-}$ mice. Flow cytometric analysis of untreated lymphocytes from spleen and lymph nodes from 12-month-old control (+/+, gray) or p66Shc$^{-/-}$ (−/−, black) mice stained with the indicated cells surface markers. (A, top) Representative fluorescence-activated cell sorting (FACS) profiles of CD3/CD22 and CD4/CD8 labeling of lymphocytes from spleen (left) and lymph nodes (right). The percentage of cells that falls into the indicated quadrants is indicated. (Bottom) Histograms displaying the mean values (± SD) are shown below. For each sample, fluorescence was analyzed on gated cells with forward and side light scatter properties of lymphocytes ($n \geq 6$). (B,C) Representative FACS profiles of CD3/CD69, CD3/CD25, and CD22/CD69 labeling of lymphocytes from spleen (B) and lymph nodes (C). Histograms show the percentage (mean values ± SD) of CD69$^+$ or CD25$^+$ T cells and of CD69$^+$ B cells ($n \geq 6$; $^*P < .05$; $^{**}P < .01$; $^{***}P < .001$).

splenocytes showed that this increase affected solely mature ($IgM^{low}IgD^{high}$) but not immature (T1 and T2) B cells (Figure S1B). Similar alterations in the proportions of T and B cells were observed in lymph nodes (Figure 2A right) and peripheral blood (data not shown) from aged mice. Both males and females exhibited similar features.

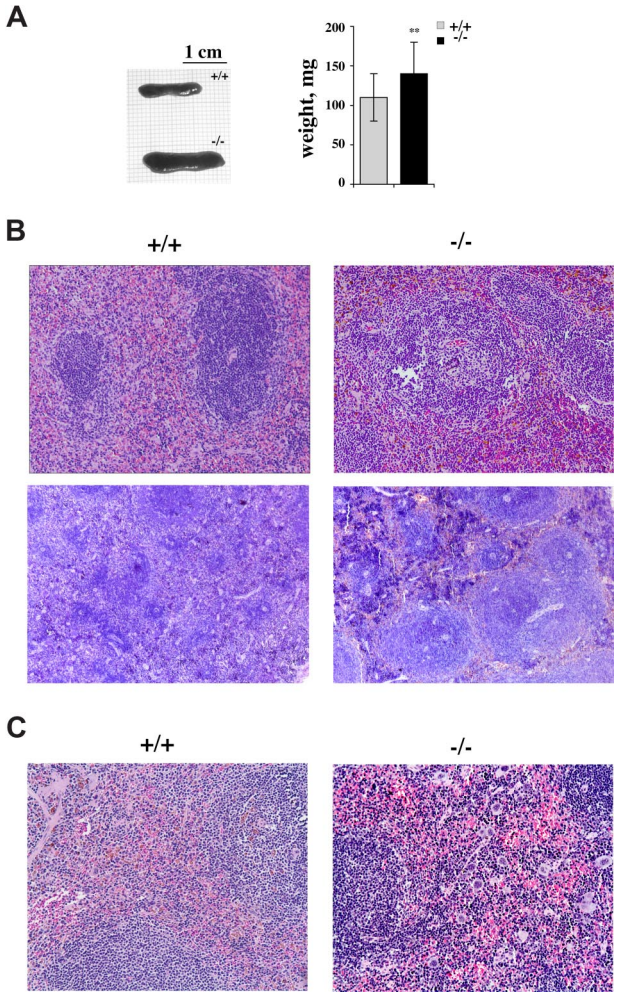

Figure 3. Splenomegaly and white and red pulp expansion in p66Shc$^{-/-}$ mice. (A) Representative image of spleen from age-matched control (+/+) or p66Shc$^{-/-}$ (−/−) mice (left) and histogram showing the weight mean values (± SD; control, gray; p66Shc$^{-/-}$, black; right). Note the significant increase in size of the mutant spleen in p66Shc-deficient mice (n = 19; $^{**}P < .01$). (B,C) Histologic analysis of spleen tissue from 12-month-old control (+/+) or p66Shc$^{-/-}$ (−/−) mice. (B) Hematoxylin and eosin (H&E; top, 100×) and Giemsa (bottom, 50 ×) staining of spleen sections from 12-month-old control (+/+) or p66Shc$^{-/-}$ (−/−) mice showing normal architecture in wild-type mice versus white pulp hyperplasia with florid germinal centers (GCs) in p66Shc$^{-/-}$ mice (n ≥ 3). Average number of follicles per full longitudinal section (mean ± SD): 40.75 (± 14) in p66Shc$^{-/-}$ mice versus 19.75 (± 4.4) in control mice; average number of germinal centers: 12.25 (± 3.3) in p66Shc$^{-/-}$ mice versus 3.25 (± 1.1) in control mice (n = 4). Germinal centers were only sporadically observed in lymph node sections, without any significant difference between p66Shc$^{-/-}$ and control mice (not shown). (C) Histologic analysis of splenic red pulp in 12-month-old control (+/+) or p66Shc$^{-/-}$ (−/−) mice. The red pulp is characterized, in p66Shc$^{-/-}$ mice, by largely increased extramedullary hematopoiesis (note the megakaryocytes and the islands of erythropoiesis; H&E, 100×, n ≥ 3).

Age-related splenomegaly and spontaneous T- and B-cell activation and proliferation in p66Shc$^{-/-}$ mice

Beginning from approximately 6 months, p66Shc$^{-/-}$ mice were found to develop with high frequency (~80%) a mild splenomegaly (Figure 3A). Histologic examination of the enlarged spleens revealed white pulp hyperplasia, associated with the presence of numerous florid germinal centers (Figure 3B). A striking expansion of the splenic red pulp was also observed. This was accompanied by a marked increase in extramedullary hematopoiesis, as indicated by the massive presence of megakaryocytes and islands of erythropoiesis and granulopoiesis (Figure 3C).

The presence of active germinal centers in the enlarged spleens of aged p66Shc$^{-/-}$ mice is likely to result from spontaneous lymphocyte activation. A large proportion of splenic T and B cells were indeed found to be activated in p66Shc$^{-/-}$ mice, as assessed by expression of surface activation markers (Figure 2B). Furthermore, although the size of the lymph nodes was not significantly increased in p66Shc$^{-/-}$ mice, the frequency of activated T and B cells was higher compared with controls (Figure 2C).

We have previously reported that splenic T cells from p66Shc$^{-/-}$ mice have a stronger proliferative response to TCR ligation, particularly when the availability of agonist is limiting,[19] indicating that p66Shc contributes to setting the threshold of TCR signaling. To understand whether p66Shc may subserve a similar function in B cells, CD22^{+} cell proliferation in response to surface IgM cross-linking was measured by CFSE dilution on single-cell suspensions of spleens from p66Shc$^{-/-}$ and control mice. As shown in Figure 4A, the proportion of proliferating p66Shc$^{-/-}$ B cells was consistently higher than control B cells at all time points analyzed. Similar results were obtained when splenic B cells were stimulated with a combination of anti-IgM antibodies and heat-inactivated *Staphylococcus aureus* (data not shown). Of note, Erk phosphorylation following surface IgM cross-linking was found to be enhanced in p66Shc$^{-/-}$ B cells compared with B cells from control mice at all agonist concentrations tested (Figure 4B), indicating that p66Shc attenuates B-cell proliferation by inhibiting BCR signaling. Hence, p66Shc deficiency results in spontaneous lymphocyte activation and proliferation, which was found to be age-related and to affect both spleen and lymph nodes.

The finding that peripheral p66Shc$^{-/-}$ T and B cells become activated and proliferate spontaneously in vivo, and that their proliferative responses to AgR agonists are enhanced compared with controls in vitro, supports the notion that p66Shc may act as a negative regulator of immune responses. To assess this possibility, we measured antibody responses to immunization with tetanus toxoid (TT). As shown in Figure 4C, the titers of anti-TT antibodies in the sera of p66Shc$^{-/-}$ mice measured after each boost were consistently higher than in control mice, indicating a more robust B-cell response. T-cell responses were measured in a contact hypersensitivity assay, where the elicitation reaction is initiated by hapten-specific T cells recruited to the site of antigen deposition, with subsequent production of proinflammatory cytokines. Mice were sensitized by epicutaneous application of TNCB, and the ear swelling response after challenge was measured. A significant increase in the ear swelling response was observed in p66Shc$^{-/-}$ mice (Figure 4D). Collectively, the data highlight a role for p66Shc as a negative regulator of T- and B-cell activation in vivo.

Development of autoimmune glomerulopathy in p66Shc$^{-/-}$ mice

Spontaneous activation of autoreactive peripheral lymphocytes is a feature associated with the development of autoimmunity. To assess the existence of activated self-reactive cells in aged p66Shc$^{-/-}$ mice, sera were tested by ELISA for the presence of autoantibodies. Anti–double-stranded DNA (dsDNA) antibodies were found in a significant proportion of aged p66Shc$^{-/-}$ mice (> 30% vs ~ 5% in age-matched controls; Figure 5A). The presence of circulating autoantibodies correlated with the presence of splenomegaly. The proportion of peritoneal B-1a (CD5^{+}) cells, which are believed to be the source of low-affinity polyclonal autoantibodies, was also increased in p66Shc$^{-/-}$ mice

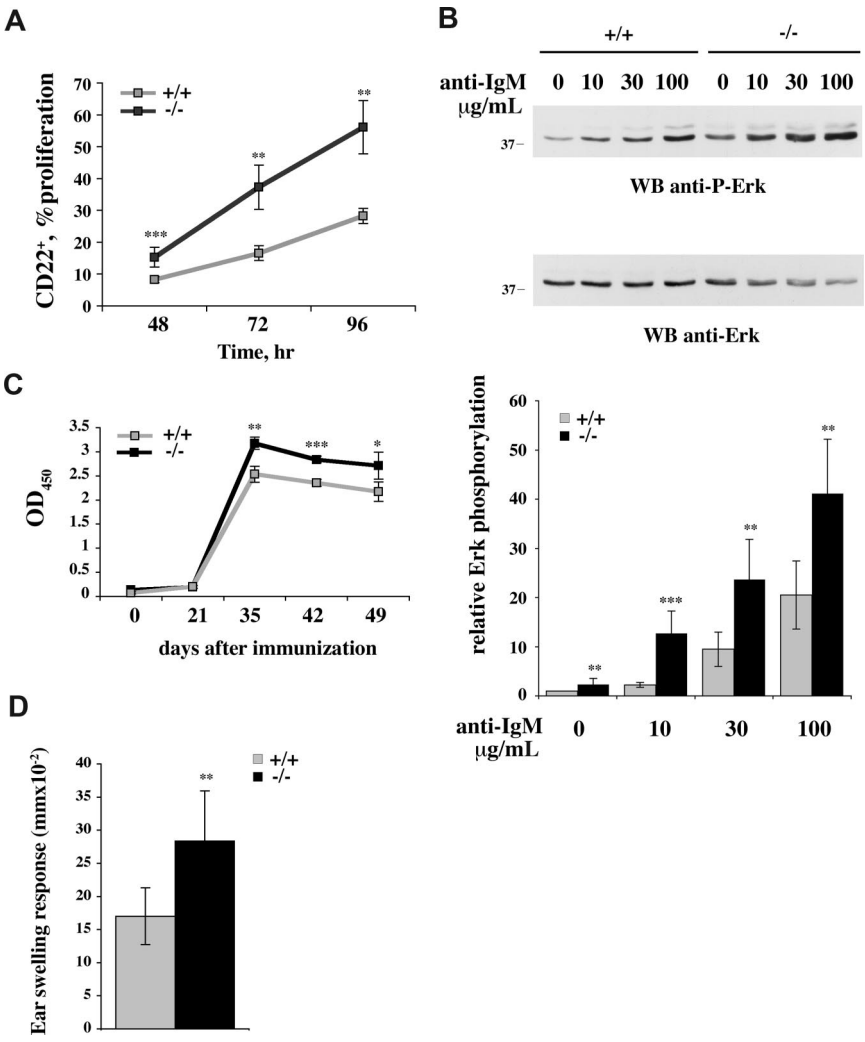

Figure 4. Enhanced lymphocyte responses in p66Shc$^{-/-}$ mice. (A) Increased proliferation of B cells from p66Shc$^{-/-}$ mice. Graph showing percentage (± SD) of proliferating splenocytes from control (+/+, gray line) or p66Shc$^{-/-}$ (−/−, black line) mice. Proliferation was analyzed by flow cytometry of CFSE-labeled cells after stimulation for 48, 72, and 96 hours with anti–mouse IgM antibodies (30 μg/mL). CFSE fluorescence was analyzed on gated CD22^{+} cells (n ≥ 3). (B, top) Enhanced BCR signaling in p66Shc$^{-/-}$ B cells. Immunoblot analysis, using a phosphospecific antibody, of Erk1/2 phosphorylation (5 minutes at 37°C) in postnuclear supernatants from splenocytes activated with the indicated concentrations of anti–mouse IgM antibodies (μg/mL). (Bottom) Quantitation by laser densitometry of the relative levels of Erk1/2 phosphorylation in splenocytes activated as described in panel B (top; n = 2, 2 mice/experiment). (C) Amplified response to tetanus toxoid immunization in p66Shc$^{-/-}$ mice. Serum samples from 6-month-old control (+/+, gray line) or p66Shc$^{-/-}$ (−/−, black line) mice immunized 4 times with 2 μg TT were collected after each immunization and anti–TT-specific antibodies were measured by ELISA. Representative data of 3 experiments (each carried out on a group of 3 mice) are shown. (D) Enhanced DTH reaction in p66Shc$^{-/-}$ mice. Control (+/+, gray) or p66Shc$^{-/-}$ (−/−, black) mice were sensitized with 3% TNCB and challenged 6 days later on one ear (TNCB 1%). Ear swelling was assessed 24 hours later and values are represented as mean of thickness of challenged ear − thickness of unchallenged ear plus or minus SD (n = 6) (*$P < .05$; **$P < .01$; ***$P < .001$).

(Figure 5B). Consistent with these autoimmune features, analysis of serum immunoglobulins revealed an increase in IgG concentrations, which involved principally the IgG1 and IgG2a isotypes (Figure 5C).

Circulating anti-dsDNA antibodies are a hallmark of lupuslike autoimmune syndromes.[22] These autoantibodies can deposit as immune complexes in kidney glomeruli through entrapment of circulating immune complexes as well as formation of immune complexes in situ following cross-reaction with components of the glomerular basement membranes, leading to complement fixation and activation. This results in tissue damage and initiation of an inflammatory process that can eventually result in the development of glomerulonephritis.[23] Kidney sections from p66Shc$^{-/-}$ and control mice were subjected to immunofluorescence analysis using fluorochrome-labeled anti–mouse IgG antibodies. As shown in Figure 6A, as opposed to glomeruli from control mice, intense granular staining was observed in glomeruli of p66Shc$^{-/-}$ mice, consistent with immune complex deposition.

Histologic analysis of p66Shc$^{-/-}$ kidneys revealed that, while glomerular size and tubular architecture were generally unaffected, glomeruli exhibited diffuse thickening of the capillary basement membranes without any significant increase in cellularity (Figure 6B). Occasional infiltration of lymphoid-like cells was observed (data not shown). Upon electron microscopic examination, glomerular basement membranes appeared coarsely and irregularly thickened, with the presence of frequent electron-dense patches, consistent with the immune complex deposits observed by immunofluorescence. Widespread effacement of foot processes was also observed, as were occasional inflammatory cells (Figure 6C and data not shown).

To address the impact of the glomerular alterations on renal function, the urine from p66Shc$^{-/-}$ mice was analyzed for the presence of proteins. Proteinuria, greater than 100 mg/dL, was observed in approximately 20% of aged p66Shc$^{-/-}$ mice (n = 15 +/+; n = 21 −/−), indicating that the glomerular damage results in compromised renal function in these mice. The levels of proteinuria were highest in mice with the most marked glomerular alterations and splenomegaly. Collectively, these pathological findings are consistent with a diagnosis of progressive autoimmune membranous glomerulonephritis in p66Shc$^{-/-}$ mice.

Spontaneous development of autoimmune alopecia in p66Shc$^{-/-}$ mice

Spontaneous alopecia is feature often associated with autoimmune diseases, including systemic lupus erythematosus (SLE). As opposed to their wild-type counterparts, aging p66Shc$^{-/-}$ mice frequently showed patches of bare skin in the absence of preexisting active lesions. Alopecia was found to initially

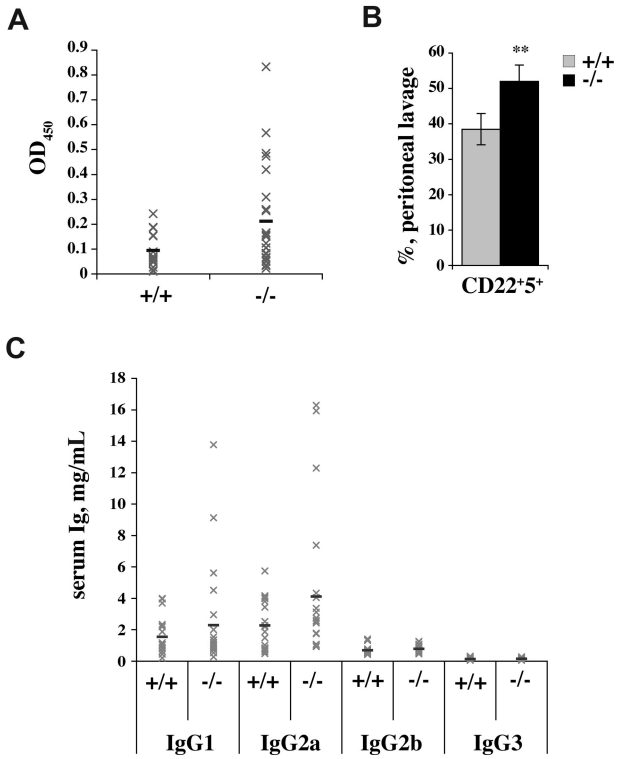

Figure 5. Autoimmune features in p66Shc$^{-/-}$ mice. (A) Autoantibody production in p66Shc$^{-/-}$ mice. Sera from 12-month-old control (+/+) or p66Shc$^{-/-}$ (−/−) mice were analyzed by ELISA for detection of anti-dsDNA antibody titers. Gray crosses show OD_{450} for each mouse analyzed, while the black lines indicate the mean values ($n \geq 16$). (B) p66Shc$^{-/-}$ mice have increased levels of B1 cells in the peritoneal cavity. Peritoneal lymphoid cells were stained with anti-CD22/anti-CD5 fluorochrome-conjugated mAb. The bar graph shows the percentage ± SD of $CD22^+CD5^+$ cells in peritoneal lavages of control (gray) and p66Shc$^{-/-}$ mice (black) ($n \geq 4$; $^{**}P < .01$). (C) Elevated serum IgG1 and IgG2a in p66Shc$^{-/-}$ mice. Levels of IgG isotypes in the serum from 12-month-old wild-type (+/+) and p66Shc-deficient (−/−) mice were measured by ELISA. Gray crosses show IgG concentration (mg/mL) for each mouse analyzed, while the black lines indicated the mean values ($n \geq 20$).

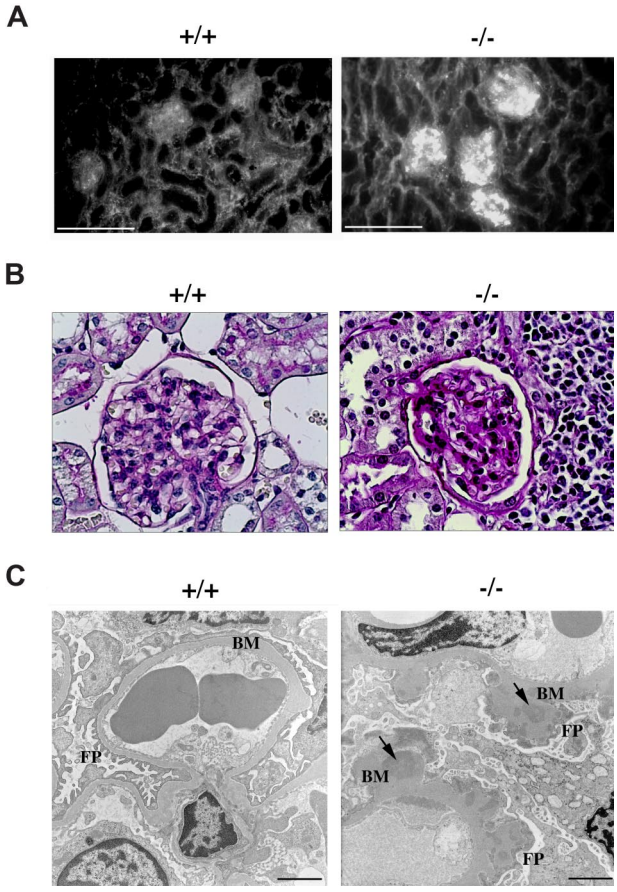

Figure 6. p66Shc$^{-/-}$ mice develop glomerulonephritis. Immunofluorescence, periodic acid-Schiff (PAS) staining, electronic microscopy of kidney from 12-month-old control (+/+) or p66Shc$^{-/-}$ (−/−) mice. (A) Ig analysis by fluorescence staining with FITC-conjugated anti–mouse IgG reveals immune complexes diffusely deposited in the glomeruli of kidneys from p66Shc$^{-/-}$ mice not observed in controls. Scale bar represents 100 μm ($n \geq 7$). (B) Histology of PAS-stained kidney sections shows normocellular glomerulus in wild-type mice and diffuse increase in thickening of glomerular basal membrane in p66Shc$^{-/-}$ mice (400×, $n \geq 3$). (C) Ultrastructural analysis of uranyl acetate–stained frozen kidney sections by transmission electron microscopy shows thickening of glomerular basement membranes (BM) in p66Shc$^{-/-}$ mice versus controls. The external face of the basement membranes of p66Shc$^{-/-}$ glomeruli appears coarse and irregular, with a clear effacement of foot processes (FPs). Electron dense patches within the thickness of the basement membranes represent immune complex deposits (▲). Scale bar represents 2 μm ($n \geq 14$).

involve the scalp and subsequently the back, and to preferentially affect females (Figure 7A). Histologic examination of skin sections showed that the dermal layer was significantly thinner in alopecic skin areas of p66Shc$^{-/-}$ mice compared with normal skin areas in these mice, as well as in age- and sex-matched controls (Figure 7B and data not shown). Furthermore, the connective components of the dermis appeared looser in alopecic skin areas, consistent with the presence of edema, as also suggested by the dermal morphology observed in toluidine-stained sections (Figure 7C). Hair follicles and sebaceous glands appeared atrophic and reduced in numbers, accounting for the alopecia. Massive lymphatic infiltration was frequently observed around and within these structures (Figure 7B inset), suggesting autoimmune destruction of the hair follicles. Toluidine blue staining of skin sections revealed the presence of numerous mast cells infiltrated in the dermis of alopecic skin areas of p66Shc$^{-/-}$ mice (Figure 7C). In agreement with the presence of edema, electron microscopic analysis showed that infiltrated p66Shc$^{-/-}$ mast cells were activated, as indicated by the presence of large numbers of granules, which in some instances appeared to be releasing their contents to the extracellular space (Figure 7C insets).

Although their pathological role is as yet debated, deposition of immune complexes in autoimmune skin lesions, resulting from recognition of self- or cross-reactive antigens, has been described.[24] To assess the potential presence of immune complex deposits in the skin of p66Shc$^{-/-}$ mice, frozen sections were subjected to immunofluorescence analysis using fluorochrome-labeled anti–mouse IgG antibodies. Intense diffuse dermal staining was observed in alopecic skin areas of p66Shc$^{-/-}$ mice, consistent with immune complex deposition (Figure 7D). The presence of circulating autoantibodies against skin antigens was further supported by the finding that sera from p66Shc$^{-/-}$ mice showed immunoreactivity to the skin of control mice (Figure S2). Taken together with the lymphatic infiltration of hair follicles and the presence of activated mast cells, which are found in skin lesions in a number of autoimmune diseases and are believed to play a role in autoimmunity,[25] this result supports an autoimmune etiology for the skin alterations observed in p66Shc$^{-/-}$ mice.

Discussion

By acting as scaffolds in AgR signaling, adaptors are critically implicated in lymphocyte development and homeostasis.[26] In

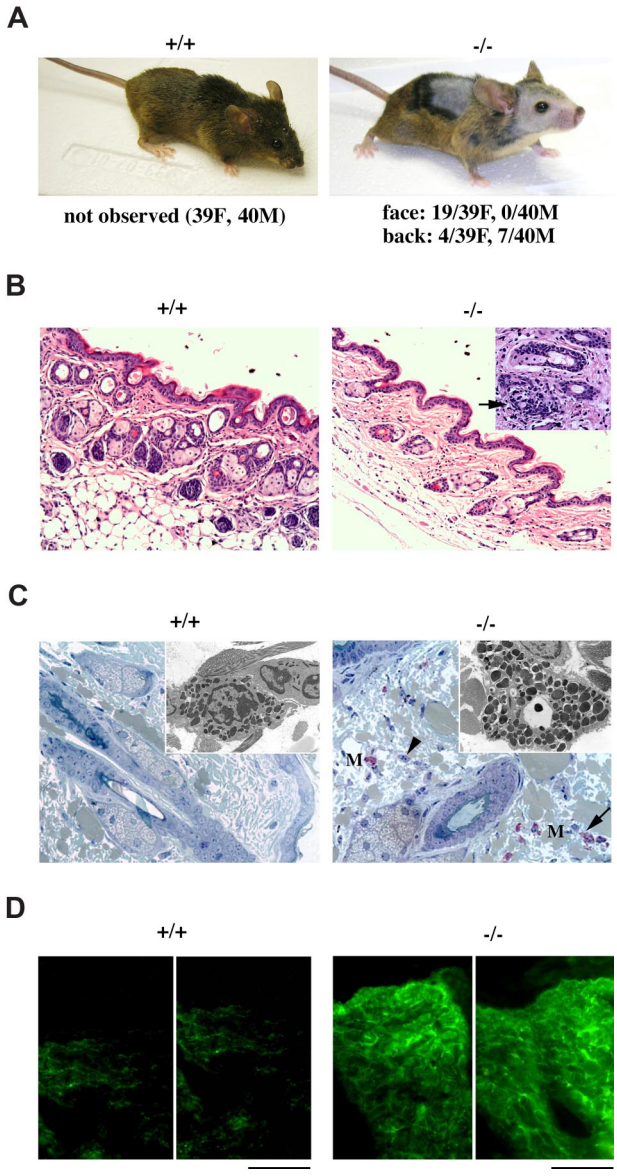

Figure 7. p66Shc$^{-/-}$ mice develop lupus-like alopecia. (A) Representative pictures of control (+/+) and p66Shc$^{-/-}$ (−/−) mice with alopecia. At the bottom, the frequencies of alopecia in the face and scalp or in the back of female (F) and male (M) mice are reported. The incidence of the lesions was not affected by the number of mice per cage. No microorganisms were found by either light or electron microscopy. (B) Histologic analysis of skin sections. H&E stained shows thinning of dermis and reduction in size and number of hair follicles in p66Shc$^{-/-}$ mice (100×). The inset shows lymphatic infiltration around and within the hair follicles (arrow) (200×) ($n \geq 3$). (C) Toluidine blue–stained skin sections display numerous infiltrated mast cells (magenta, M) in p66Shc$^{-/-}$ mice versus controls (200×). The arrow indicates a degranulating mast cell. The arrowhead shows an infiltrated neutrophil. Loosening of dermal collagen fibers due to edema can be observed. The inset shows an electronic micrograph of an activated mast cell in an alopecic skin section from a p66Shc$^{-/-}$ mouse, characterized by the presence of abundant large granules throughout the cytoplasm, some of which appear to be releasing their contents to the extracellular space ($n \geq 3$). (D) Analysis of Ig deposit by fluorescence staining with FITC-conjugated goat anti–mouse immunoglobulins displays immune complexes deposited in the dermal layer of the skin from p66Shc$^{-/-}$ mice. Scale bar represents 100 μm ($n \geq 4$).

agreement with their function as attenuators of AgR signaling, deficiency of inhibitory adaptors may result in spontaneous development of autoimmune pathologies or increased susceptibility to experimentally induced autoimmunity in the mouse, as described for Cbl-b, SIT, LAT^{Y136}, or LAB.[27-31] Our data show that aging p66Shc$^{-/-}$ mice spontaneously develop a systemic lupus-like autoimmune disease, characterized by spontaneous peripheral T- and B-cell activation and hyperresponsiveness to AgR engagement both in vitro and in vitro, thereby identifying p66Shc as an inhibitory adaptor implicated in the control of lymphocyte tolerance and homeostasis.

We had previously reported that p66Shc inhibits TCR coupling to Ras activation, an activity likely to account for the enhanced proliferative response of p66Shc$^{-/-}$ splenic T cells to TCR agonists, particularly evident at limiting ligand concentrations.[19] A lower activation threshold has been causally linked to spontaneous T-cell activation and systemic autoimmunity, as documented for example in GADD45α$^{-/-}$[32] or Cbl-b$^{-/-}$ mice.[27] Furthermore, CD4$^+$ T cells from lupus-prone mice are hyperresponsive to TCR stimulation with both high- and low-affinity peptide ligands.[33] A lower TCR activation threshold may therefore result in hyperresponsiveness to repeated encounters with self-antigen of the rare peripheral self-reactive p66Shc$^{-/-}$ T cells that have escaped negative selection in the thymus, leading to their gradual accumulation. This would result in breaking of peripheral tolerance and manifestation of the autoimmune phenotype. Of note, the number of regulatory T cells (Foxp3$^+$CD4$^+$) in the spleen was not affected by p66Shc deficiency (F.F., unpublished results, September 2007), ruling out the possibility that p66Shc may indirectly exert a negative control on peripheral autoreactive T-cell activation by promoting regulatory T-cell development, as described for LAT.[34]

The proapoptotic activity of p66Shc may also contribute to explain the splenomegaly observed in aged p66Shc$^{-/-}$ mice. p66Shc deficiency results indeed in impaired T-cell apoptosis[19] and may therefore favor the survival of activated self-reactive T cells. A similar dual role in the control of T-cell homeostasis has been proposed for the lipid kinase PTEN, the adaptors TSAd and LAT (Y136), and GADD45β. Peripheral T cells from *Pten*$^{+/-}$ mice, as well as from TSAd$^{-/-}$ or GADD45β$^{-/-}$ mice, or from knockin mice expressing LAT^{Y136F} display indeed a more robust proliferative response to TCR agonists and are more resistant to AICD compared with their wild-type counterparts, which results in spontaneous development of lymphoproliferative disease and systemic autoimmunity.[29,30,35-37] Although thymic development appears normal in p66Shc$^{-/-}$ mice, and p66Shc is expressed at lower levels in the thymus than in peripheral lymphoid organs, p66Shc$^{-/-}$ thymocytes are more resistant to apoptosis than their wild-type counterparts.[19] We cannot exclude that, in addition to its effects on peripheral T cells, p66Shc might also affect thymocyte survival, thereby facilitating escape of self-reactive T cells to the periphery.

The data presented here show that p66Shc plays an important role in the negative control not only of T-cell but also of B-cell activation. Peripheral p66Shc$^{-/-}$ B cells display a spontaneously activated phenotype in vivo, consistent with the presence of active germinal centers in the spleen of p66Shc$^{-/-}$ mice, and a more robust proliferative response to BCR cross-linking in vitro. Antibody responses to immunization were also enhanced in p66Shc$^{-/-}$ mice. By providing B-cell help, the hyperreactive p66Shc$^{-/-}$ T cells are very likely to contribute to the enhanced B-cell response, including activation of self-reactive B cells that present self-antigens associated with MHCII, which would result in the accumulation of circulating autoantibodies. However, the finding that p66Shc$^{-/-}$ B-cell proliferation in response to surface Ig cross-linking is enhanced indicates a direct activity of p66Shc in controlling mitogenic signaling in B cells. This notion is supported by the enhancement in BCR-dependent Erk

phosphorylation in p66Shc$^{-/-}$ B cells. p52Shc is implicated in coupling the BCR to Ras activation through binding to phosphorylated Igα/Igβ and recruitment of Grb2/Sos complexes close to Ras at the plasma membrane.[38] The finding that p66Shc acts a dominant inhibitor of p52Shc in T cells[19] suggests that a similar mechanism, involving p66Shc/p52Shc competition for binding to Igα/Igβ, might be operational in B cells.

p66Shc$^{-/-}$ mice spontaneously develop with age systemic autoimmunity. Pathological features include (1) lymphoid hyperplasia, characterized by active germinal centers in the spleen and accumulation of spontaneously activated lymphocytes, which are more resistant to AICD when tested ex vivo; (2) increased Ig, with a preferential increase in IgG2a isotypes, which have been implicated in the disease for their capacity to efficiently activate complement and interact with FcγRI/FcγRIII[39]; (3) production of antibodies against dsDNA, the principal self-antigen in SLE[22]; (4) glomerular immune complex deposition, with basement membrane thickening and development of membranous glomerulonephritis; and (5) alopecia, affecting preferentially females, characterized by dermal deposition of immune complexes, follicular infiltration of lymphoid cells, and presence of activated mast cells. With the possible exception of alopecia, all other features are consistent with a lupus-like autoimmune syndrome.[22] Patchy nonscarring alopecia, characterized by decrease in hair follicle density associated with lymphatic infiltration of the follicle and lack of superficial inflammation, is among the cutaneous presentations of SLE.[24] Furthermore, activated mast cells in the dermis are a feature of murine cutaneous SLE.[40] On the other hand, at variance with our observations, epidermal thickening and localized immune complex deposition at the dermal-epidermal junction are found in murine SLE.[41] While these differences require further investigation, the massive dermal deposition of immune complexes in alopecic p66Shc$^{-/-}$ skin areas is likely to be causal to the development of alopecia by promoting FcRγIII-dependent mast cell activation.[25] This would result in leukocyte and lymphocyte infiltration, ultimately leading to autoimmune attack of hair follicles by autoreactive/cross-reactive T cells.

Lupus-like autoimmune disease has been associated with loss of proapoptotic proteins, including proapoptotic Bcl-2 family members,[42,43] Fas/FasL,[44] and proteins involved in p53-dependent apoptosis.[32,37,45] p66Shc has been implicated in the latter pathway in fibroblasts.[6,15] Furthermore, p66Shc overexpression in T cells correlates with increased levels of the p53 effector, GADD45α.[19] Lupus-like autoimmunity has also been described in mice deficient for or expressing mutated versions of a number of components of the AgR signaling machinery, including kinases,[35,46] phosphatases,[47-49] and adaptors.[27,29-31,36] Our findings implicate p66Shc not only as a regulator of apoptosis, but as an important participant in the inhibitory circuitry responsible for fine-tuning of the signals emanated from AgRs. Of note, human *ShcA* has been mapped to chromosome 1q21, where a susceptibility locus for SLE,[50] as well as for other autoimmune pathologies, including multiple sclerosis[51] and type-2 diabetes,[52] has been identified. The mouse syntenic region on chromosome 3 also displays susceptibility loci in multiple autoimmune disease models, including *Eae3, Idd10,* and *Idd17*.[53] To date, only 2 rare polymorphisms in the p66Shc gene are known, mapping to the gene promoter.[54] It will be of interest to analyze *ShcA* for the presence of polymorphisms in SLE patients, to address its potential role as a susceptibility gene in this disease.

Our finding that p66Shc is expressed in monocytes, together with the increased extramedullary hematopoiesis observed in the spleen, suggests that p66Shc may play a role not only in the lymphoid but also in the myeloid compartment. p52Shc participates in signaling by FcRs.[55] By transdominantly inhibiting p52Shc, which we have shown to control endocytosis in T cells,[8] p66Shc may impair internalization of immune complexes by FcRs and subsequent processing and presentation of internalized antigen. If this is the case, antigen presentation might be enhanced in p66Shc$^{-/-}$ mice, including presentation of self-antigen bound to autoantibodies that, together with the lower TCR activation threshold, would promote expansion of self-reactive T cells. p52Shc has also been implicated in signaling by receptors of hematopoietic growth factors, including Epo, IL-3, and granulocyte-macrophage colony-stimulating factor (GM-CSF).[56,57] Since p66Shc$^{-/-}$ mice were neither anemic nor neutropenic, nor was any abnormality detected upon histologic analysis of the bone marrow (F.F., unpublished observations, February 2008), we could hypothesize that the extramedullary hematopoiesis is not a compensatory response, but rather that hematopoietic precursors in the spleen of these mice respond more vigorously to growth factors because p52Shc is not inhibited by p66Shc. On the other hand, activated peripheral T cells have been shown to produce IL-3 and GM-CSF,[58] 2 cytokines that promote hematopoiesis. A local increase in production of these cytokines by activated T cells may favor the development of hematopoietic precursors in the spleen of p66Shc$^{-/-}$ mice.

A closing issue is why the pathology observed in p66Shc$^{-/-}$ mice is generally less severe than in mice deficient in other inhibitory adaptors,[27-31] as well as in the classical MRL/lpr model of murine lupus.[44] The onset of autoimmunity, albeit spontaneous, is indeed late in p66Shc$^{-/-}$ mice. Furthermore, notwithstanding their pathological features, including glomerulopathy, p66Shc$^{-/-}$ mice have a prolonged life span.[15] How the genetic background may affect expression of the disease is an important issue to be addressed. The ROS-enhancing activity of p66Shc may, however, contribute to the relatively mild disease manifestations in p66Shc$^{-/-}$ mice. The reduction in ROS production in p66Shc$^{-/-}$ mice results indeed in a higher resistance to oxidative stress–related diseases, such as high-fat diet–induced atherogenesis[16] and diabetic glomerulopathy.[17] We can speculate that, once chronic inflammation develops as the result of glomerular immune complex deposition, the reduction in ROS production by glomerular cells and infiltrated phagocytes may protect the kidney from injury and thereby delay oxidative stress-related tissue damage. In this scenario, it is interesting to speculate as to the evolutionary advantage of conserving a gene that promotes apoptosis and aging, and favors development of oxidative stress–related diseases. One obvious reason would be protection from cancer, resulting from accumulation of mutations in damaged or aged cells that fail to be removed by apoptosis. This does not, however, appear to apply to p66Shc, as p66Shc$^{-/-}$ mice do not develop neoplastic pathologies even at an old age.[15] Our findings suggest that the protective function of p66Shc against autoimmunity may have been a driving force in its positive selection by evolution.

Acknowledgments

The authors thank Sonia Grassini and Luigi Federico Falso for technical assistance; Stefano Feti for animal care; and Lorenzo Leoncini, Mario M. D'Elios, Andrea Cavani, and John L. Telford for productive discussions.

This work was generously supported by AIRC. The financial support of Istituto Toscano Tumori and MIUR (PRIN) is also acknowledged. F.F. and M.P. are FIRC fellows.

Authorship

Contribution: F.F., M.P., C.U., M.T.S., and C.T.B. designed research and analyzed and interpreted data; F.F., M.P., C.U., M.T.S., E.P., and C.G. performed research; L.L. and P.G.P. contributed vital reagents; C.T.B. and F.F. drafted the paper.

Conflict-of-interest disclosure: P.G.P. is a shareholder of Genextra Spa. The other authors declare no competing financial interests.

Correspondence: Cosima T. Baldari, Department of Evolutionary Biology, University of Siena, Via Aldo Moro 2, 53100 Siena, Italy; e-mail: baldari@unisi.it.

References

1. Luzi L, Confalonieri S, Di Fiore PP, Pelicci PG. Evolution of Shc functions from nematode to human. Curr Opin Genet Dev. 2000;10:668-674.
2. Fagiani E, Giardina G, Luzi L, et al. RaLP, a new member of the Src homology and collagen family, regulates cell migration and tumor growth of metastatic melanomas. Cancer Res. 2007;67:3064-3073.
3. Migliaccio E, Mele S, Salcini AE, et al. Opposite effects of the p52shc/p46shc and p66shc splicing isoforms on the EGF receptor-MAP kinase-fos signalling pathway. EMBO J. 1997;16:706-716.
4. Giorgio M, Migliaccio E, Orsini F, et al. Electron transfer between cytochrome c and p66Shc generates reactive oxygen species that trigger mitochondrial apoptosis. Cell. 2005;122:221-233.
5. Ventura A, Luzi L, Pacini S, Baldari CT, Pelicci PG. The p66Shc longevity gene is silenced through epigenetic modifications of an alternative promoter. J Biol Chem. 2002;277:22370-22376.
6. Trinei M, Giorgio M, Cicalese A, et al. A p53-p66Shc signalling pathway controls intracellular redox status, levels of oxidation-damaged DNA and oxidative stress–induced apoptosis. Oncogene. 2002;21:3872-3878.
7. Ravichandran KS. Signaling via Shc family adapter proteins. Oncogene. 2001;20:6322-6330.
8. Patrussi L, Ulivieri C, Lucherini OM, et al. p52SHC is required for CXCR4-dependent signaling and chemotaxis in T-cells. Blood. 2007;110:1730-1738.
9. Ventura A, Maccarana M, Raker VA, Pelicci PG. A cryptic targeting signal induces isoform-specific localization of p46Shc to mitochondria. J Biol Chem. 2004;279:2299-2306.
10. Pellegrini M, Pacini S, Baldari CT. p66SHC: the apoptotic side of Shc proteins. Apoptosis. 2005;10:13-18.
11. Pinton P, Rimessi A, Marchi S, et al. Protein kinase C beta and prolyl isomerase 1 regulate mitochondrial effects of the life-span determinant p66Shc. Science. 2007;315:659-663.
12. Orsini F, Migliaccio E, Moroni M, et al. The life span determinant p66Shc localizes to mitochondria where it associates with mitochondrial heat shock protein 70 and regulates transmembrane potential. J Biol Chem. 2004;279:25689-25695.
13. Nemoto S, Finkel T. Redox regulation of forkhead proteins through a p66shc-dependent signaling pathway. Science. 2002;295:2450-2452.
14. Nemoto S, Combs CA, French S, et al. The mammalian longevity-associated gene product p66shc regulates mitochondrial metabolism. J Biol Chem. 2006;281:10555-10560.
15. Migliaccio E, Giorgio M, Mele S, et al. The p66shc adaptor protein controls oxidative stress response and life span in mammals. Nature. 1999;402:309-313.
16. Napoli C, Martin-Padura I, de Nigris F, et al. Deletion of the p66Shc longevity gene reduces systemic and tissue oxidative stress, vascular cell apoptosis, and early atherogenesis in mice fed a high-fat diet. Proc Natl Acad Sci U S A. 2003;100:2112-2116.
17. Menini S, Amadio L, Oddi G, et al. Deletion of p66Shc longevity gene protects against experimental diabetic glomerulopathy by preventing diabetes-induced oxidative stress. Diabetes. 2006;55:1642-1650.
18. Pezzicoli A, Ulivieri C, Capitani N, Ventura A, Pelicci P, Baldari CT. Expression in T-cells of the proapoptotic protein p66SHC is controlled by promoter demethylation. Biochem Biophys Res Commun. 2006;349:322-328.
19. Pacini S, Pellegrini M, Migliaccio E, et al. p66SHC promotes apoptosis and antagonizes mitogenic signaling in T cells. Mol Cell Biol. 2004;24:1747-1757.
20. Pellegrini M, Finetti F, Petronilli V, et al. p66SHC promotes T cell apoptosis by inducing mitochondrial dysfunction and impaired Ca2+ homeostasis. Cell Death Differ. 2007;14:338-347.
21. Dieli F, Sireci G, Scire E, Salerno A, Bellavia A. Impaired contact hypersensitivity to trinitrochlorobenzene in interleukin-4-deficient mice. Immunology. 1999;98:71-79.
22. Singh RR. SLE: translating lessons from model systems to human disease. Trends Immunol. 2005;26:572-579.
23. Nangaku M, Couser WG. Mechanisms of immune-deposit formation and the mediation of immune renal injury. Clin Exp Nephrol. 2005;9:183-191.
24. Trueb RM. Hair and nail involvement in lupus erythematosus. Clin Dermatol. 2004;22:139-147.
25. Benoist C, Mathis D. Mast cells in autoimmune disease. Nature. 2002;420:875-878.
26. Koretzky GA, Myung PS. Positive and negative regulation of T-cell activation by adaptor proteins. Nat Rev Immunol. 2001;1:95-107.
27. Bachmaier K, Krawczyk C, Kozieradzki I, et al. Negative regulation of lymphocyte activation and autoimmunity by the molecular adaptor Cbl-b. Nature. 2000;403:211-216.
28. Simeoni L, Posevitz V, Kolsch U, et al. The transmembrane adapter protein SIT regulates thymic development and peripheral T-cell functions. Mol Cell Biol. 2005;25:7557-7568.
29. Aguado E, Richelme S, Nunez-Cruz S, et al. Induction of T helper type 2 immunity by a point mutation in the LAT adaptor. Science. 2002;296:2036-2040.
30. Sommers CL, Park CS, Lee J, et al. A LAT mutation that inhibits T cell development yet induces lymphoproliferation. Science. 2002;296:2040-2043.
31. Zhu M, Koonpaew S, Liu Y, et al. Negative regulation of T cell activation and autoimmunity by the transmembrane adaptor protein LAB. Immunity. 2006;25:757-768.
32. Salvador JM, Hollander MC, Nguyen AT, et al. Mice lacking the p53-effector gene Gadd45a develop a lupus-like syndrome. Immunity. 2002;16:499-508.
33. Vratsanos GS, Jung S, Park YM, Craft J. CD4(+) T cells from lupus-prone mice are hyperresponsive to T cell receptor engagement with low and high affinity peptide antigens: a model to explain spontaneous T cell activation in lupus. J Exp Med. 2001;193:329-337.
34. Koonpaew S, Shen S, Flowers L, Zhang W. LAT-mediated signaling in CD4+CD25+ regulatory T cell development. J Exp Med. 2006;203:119-129.
35. Di Cristofano A, Kotsi P, Peng YF, Cordon-Cardo C, Elkon KB, Pandolfi PP. Impaired Fas response and autoimmunity in Pten+/- mice. Science. 1999;285:2122-2125.
36. Drappa J, Kamen LA, Chan E, et al. Impaired T cell death and lupus-like autoimmunity in T cell-specific adapter protein-deficient mice. J Exp Med. 2003;198:809-821.
37. Liu L, Tran E, Zhao Y, Huang Y, Flavell R, Lu B. Gadd45 beta and Gadd45 gamma are critical for regulating autoimmunity. J Exp Med. 2005;202:1341-1347.
38. D'Ambrosio D, Hippen KL, Cambier JC. Distinct mechanisms mediate SHC association with the activated and resting B cell antigen receptor. Eur J Immunol. 1996;26:1960-1965.
39. Schmidt RE, Gessner JE. Fc receptors and their interaction with complement in autoimmunity. Immunol Lett. 2005;100:56-67.
40. Nishimura H, Strominger JL. Involvement of a tissue-specific autoantibody in skin disorders of murine systemic lupus erythematosus and autoinflammatory diseases. Proc Natl Acad Sci U S A. 2006;103:3292-3297.
41. Horiguchi Y, Furukawa F, Hamashima Y, Imamura S. Ultrastructural lupus band test in the skin of MRL mice. Arch Dermatol Res. 1986;278:474-480.
42. Bouillet P, Metcalf D, Huang DC, et al. Proapoptotic Bcl-2 relative Bim required for certain apoptotic responses, leukocyte homeostasis, and to preclude autoimmunity. Science. 1999;286:1735-1738.
43. Takeuchi O, Fisher J, Suh H, Harada H, Malynn BA, Korsmeyer SJ. Essential role of BAX,BAK in B cell homeostasis and prevention of autoimmune disease. Proc Natl Acad Sci U S A. 2005;102:11272-11277.
44. Cohen PL, Eisenberg RA. Lpr and gld: single gene models of systemic autoimmunity and lymphoproliferative disease. Annu Rev Immunol. 1991;9:243-269.
45. Zheng SJ, Lamhamedi-Cherradi SE, Wang P, Xu L, Chen YH. Tumor suppressor p53 inhibits autoimmune inflammation and macrophage function. Diabetes. 2005;54:1423-1428.
46. Nishizumi H, Taniuchi I, Yamanashi Y, et al. Impaired proliferation of peripheral B cells and indication of autoimmune disease in lyn-deficient mice. Immunity. 1995;3:549-560.
47. Tsui HW, Siminovitch KA, de Souza L, Tsui FW. Motheaten and viable motheaten mice have mutations in the haematopoietic cell phosphatase gene. Nat Genet. 1993;4:124-129.
48. Majeti R, Xu Z, Parslow TG, et al. An inactivating point mutation in the inhibitory wedge of CD45 causes lymphoproliferation and autoimmunity. Cell. 2000;103:1059-1070.
49. Moody JL, Pereira CG, Magil A, Fritzler MJ, Jirik

FR. Loss of a single allele of SHIP exacerbates the immunopathology of Pten heterozygous mice. Genes Immun. 2003;4:60-66.

50. Shen N, Tsao BP. Current advances in the human lupus genetics. Curr Rheumatol Rep. 2004;6:391-398.
51. Dai KZ, Harbo HF, Celius EG, et al. The T cell regulator gene SH2D2A contributes to the genetic susceptibility of multiple sclerosis. Genes Immun. 2001;2:263-268.
52. Das SK, Hasstedt SJ, Zhang Z, Elbein SC. Linkage and association mapping of a chromosome 1q21-q24 type 2 diabetes susceptibility locus in northern European Caucasians. Diabetes. 2004; 53:492-499.
53. Marrack P, Kappler J, Kotzin BL. Autoimmune disease: why and where it occurs. Nat Med. 2001;7:899-905.
54. Sentinelli F, Romeo S, Barbetti F, et al. Search for genetic variants in the p66Shc longevity gene by PCR-single strand conformational polymorphism in patients with early-onset cardiovascular disease. BMC Genet. 2006;7:14-20.
55. Park RK, Liu Y, Durden DL. A role for Shc, Grb2, and Raf-1 in FcgammaRI signal relay. J Biol Chem. 1996;271:13342-13348.
56. He TC, Jiang N, Zhuang H, Wojchowski DM. Erythropoietin-induced recruitment of Shc via a receptor phosphotyrosine-independent, Jak2-associated pathway. J Biol Chem. 1995;270: 11055-11061.
57. Matsuguchi T, Salgia R, Hallek M, et al. Shc phosphorylation in myeloid cells is regulated by granulocyte macrophage colony-stimulating factor, interleukin-3, and steel factor and is constitutively increased by p210BCR/ABL. J Biol Chem. 1994;269:5016-5021.
58. Sharara LI, Andersson A, Guy-Grand D, Fischer A, DiSanto JP. Deregulated TCR alpha beta T cell population provokes extramedullary hematopoiesis in mice deficient in the common gamma chain. Eur J Immunol. 1997;27:990-998.